Anisotropic Radiation Damage of Nuclear Grade Beryllium for Research Reactor Application

Suk Hoon Kang [*,a], Jinsung Jang [a], Young-Bum Chun [a], Sanghoon Noh [a], Yong Hwan Jeong [a], Tae Kyu Kim [a]

[a] *Nuclear Materials Division, Korea Atomic Energy Research Institute, Daejeon 305-353*

1. Introduction

Pure beryllium has a very low mass absorption coefficient, and has been used as the reflector element material in research reactors. The lifetime of beryllium reflector elements are usually determined by the radiation induced swelling [1-4]; the swelling leads to a directional change in the reflector frame, which results in the bending or cracking of the reflector parts. Therefore, the accumulation of radiation data is very important to answer the life time of the material, and a visualization of the microstructure evolution during radiation is helpful to understand the right material usages. Ion irradiation is widely used as means of introducing radiation damage in materials [5,6]. Protons can be used to simulate the effects of the neutron irradiation on the material since the mass of protons and neutrons is very similar (1.007amu). Protons are large and heavy like neutrons; the only difference is that they have a positive charge. The corresponding irradiation characteristic difference between protons and neutrons is definite; irradiated protons will be stopped inside the target material because of the electron stopping power, while irradiated neutrons penetrate the target material [7,8]. However, it is suspected that the microstructure evolution during a nuclear stopping event will be similar between the proton and neutron irradiation, when the mass difference between an incident ion and target atom is relatively small. It is expected that beryllium atoms will actively react with the protons because they also have a relatively low atomic mass (9.012 amu). The displacement of beryllium atoms will cause the accumulation of vacancies; this is very harmful to metals because of its strong interaction with lattice defects. As a result, local swelling and degradation of mechanical properties of bulk materials take place as well.

In this study, the evolutions of proton induced damages were visualized, and anisotropic distribution of vacancies in a beryllium sample was investigated. It was typically observed that the evolutions of vacancies were affected by the grain orientation rather than the irradiation direction.

2. Methods and Results

A column of loose beryllium powder (98.5%) was compacted under a vacuum hot pressing (VHP) which operates in the vacuum by the pressure of the opposed upper and lower punches, bringing the billet to its final density. The VHP processed commercial grade beryllium (S-200-F) was sliced into a 1cm X 1cm square sheet. The surface of the sheet was mechanically polished with diamond paste, and then electro-polished by 10% perchloric acid. The microstructure of beryllium was observed by electron backscattered diffraction (EBSD, JSM 6500F & INCA system), and the grain size and preferred orientations were estimated. The electro-polished surface was irradiated by protons at room temperature; the acceleration voltage and proton amounts were 120keV, and 2.0×10^{18} ions/cm^2, respectively. A TEM sample of a proton-irradiated beryllium sample was manufactured using a focused ion beam (FIB, NOVA200). The microstructure evolution during proton irradiation has been observed by bright field image and selective area diffraction pattern (SADP) of TEM (JSM 2100F). The collision depths of protons on the beryllium surface were estimated using a molecular dynamics simulation code, SRIM2012. The estimated collision depth was compared with the TEM observation.

In figure 1, the microstructure of a beryllium reflector block (S-200-F) was observed using EBSD. A SEM image of etched surface is shown in figure 1(a), an EBSD band contrast is shown in 1(b), and a crystal orientation map is shown in 1(c). In figure 1(a), deep furrows were observed at the grain boundaries, and the furrows were developed during electro polishing of sample surface by 10% perchloric acid. The etchant preferentially attacked the interface between beryllium and BeO. It was suspected that the dip furrow was the place where the BeO particles were located. In figure 1(b), the band contrast (BC) map of beryllium is introduced, which is a qualitative factor of an EBSD. It is derived from the intensity of the diffraction bands; it shows detailed features of the microstructure such as the grain boundaries.

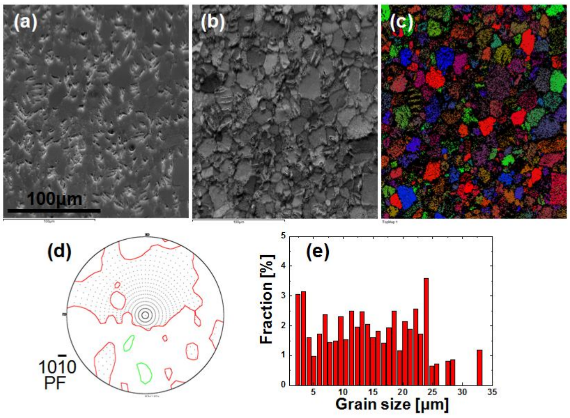

Fig. 1. Microstructure of a beryllium reflector block (S-200-F). The grain shapes are shown through a (a) SEM image of the etched surface, (b) the EBSD band contrast, and (c) a crystal orientation map, respectively. A corresponding (d) $10\bar{1}0$ polefigure and (e) the grain size distributions are shown.

The shape of the grains also can be observed in the grain map. Figure 1(c) shows the different colors of each grain; the blue, red, and green colors suggest that the grains have different crystallographic orientations. The random orientation distribution of the beryllium sample is confirmed in the pole figure. In figure 1(d), a $10\bar{1}0$ pole figure of the beryllium sample has been measured by EBSD, and the results show that there was no special preferred orientation. It can be concluded that the VHP process was quite effective to produce a beryllium reflector block of random orientation. In figure 1(e), the grain size distribution of a beryllium sample has been measured, and the result shows that the grains are homogeneous, and the average size is estimated to be less than 20μm. After the EBSD observation, the sample was irradiated by protons.

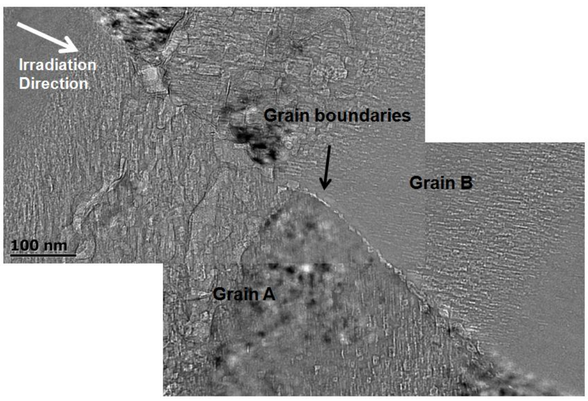

Fig. 2. Cross-section image of proton irradiated (120 keV, 2.0×10^{18} ions/cm^2) beryllium, observed by TEM. Two different grains (Grain A and B) are irradiated simultaneously. The distribution of vacancies was affected by the crystal orientation and grain boudaries.

In figure 2, proton irradiation has been carried out at 120keV and 2.0×10^{18} ions/cm^2. A cross-section image of proton irradiated beryllium was observed by TEM. Various sizes of vacancies were developed in the damaged area; the largest vacancies were observed at a 600nm in depth, and the other small vacancies were distributed up to 1μm in depth. In the irradiation damaged area between 600~1000 nm, a grain boundary was clearly observed, and two different grains (Grain A and B) were irradiated simultaneously. It was typically observed that the distribution of vacancies was affected by the crystal orientation and grain boundaries. Grains A and B showed different directions of vacancies alignment, which was common in the most severely damaged area. The selective area diffraction pattern (SADP) of TEM showed that the arrays of multiple vacancies were considerably longer along the basal plane. The beryllium atoms could be easily dislocated by proton irradiation, while the basal plane was aligned along the perpendicular direction of the irradiation.

3. Conclusions

The effects of proton irradiation on a beryllium reflector in terms of microstructure evolution have been studied to emulate the effect of neutron irradiation. Protons were irradiated on a beryllium sample by 120 keV acceleration voltage at room temperature up to 2.0×10^{18} ions/cm^2. While the irradiated sample was observed by TEM, the most severely damaged area was located at 600 nm in depth; tens of nanometer sized vacancies were distributed. Multiple vacancies were preferentially distributed along the grain boundaries. The equi-axed vacancies of 10 nm diameter were observed in a grain boundary, and planar vacancies were observed at the interfaces. The vacancies were also distributed in the grains; it was observed that the evolutions of the vacancies were affected by the grain orientation rather than the irradiation direction.

REFERENCES

[1] V. P. Chakin, A. O. Posevin, I. B. Kupriyanov, J. Nucl. Mater. 367–370, 1377 (2007).
[2] L. L. Snead, J. Nucl. Mater. 326, 114 (2004).
[3] D. V. Andreev, V. N. Bespalov, A. Ju. Birjukov, B. A. Gurovich, P. A. Platonov, J. Nucl. Mater. 233-237, 880 (1996).
[4] J. M. Beeston, G. R. Longhurst, R. S. Wallace, and S. P. Abeln, J. Nucl. Mater. 195, 102 (1992).
[5] N. Yoshida, S. Mizusawa, R. Sakamoto, T. Muroga, Fusion Technol. 30, 798 (1996).
[6] N. Yoshida, Y. Hirooka, J. Nucl. Mater. 258-263, 173 (1998).
[7] M. Robinson, I. Torrens, Physical Review B 9, 5008 (1974).
[8] K. Beardmore, N. Gronbech-Jensen, Physical Review E 57, 7278 (1998).